Available online at www.sciencedirect.com
ScienceDirect
Journal of Photochemistry and Photobiology A: Chemistry 193 (2008) 166–177
Journal of Photochemistry and Photobiology A:Chemistry
www.elsevier.com/locate/jphotochem

Synthesis, aggregation and photoinduced electron transfer processes of cationic water-soluble 21-thia and 21-oxaporphyrins

Sangita Santra, Tushar Kanti Mukherjee, Navodit Babel, Iti Gupta, Anindya Datta *, M. Ravikanth *

Department of Chemistry, Indian Institute of Technology, Powai, Mumbai 400076, India

Received 7 March 2007; received in revised form 19 May 2007; accepted 15 June 2007
Available online 20 June 2007

Abstract

The *meso*-pyridyl 21-thia- and 21-oxaporphyrins containing three pyridyl groups at the *meso*-positions have been methylated to obtain water-soluble porphyrins. The porphyrins are highly soluble in water and the water-soluble 21-thiaporphyrins exhibit aggregation behaviour above 10^{-4} M whereas the water-soluble 21-oxaporphyrins strongly aggregate at very low concentrations (10^{-7} M). The interaction of water-soluble ionic porphyrins with ionic surfactant in aqueous solutions has been studied as a function of surfactant concentration by means of absorption, fluorescence and resonance light scattering (RLS) techniques. It has been observed that, at the initial premicellar surfactant concentration, the oppositely charged surfactant induces aggregation and above cmc these aggregates dissociates into monomeric form and gets micellised. The self- and SDS-induced aggregation of these cationic porphyrins is found to depend on the number and position of the positive charge with respect to the porphyrin core. The micellar encapsulation technique is used to promote the photoinduced electron transfer between the porphyrins and neutral aromatic amines and it has been observed that the electron transfer rate becomes slowing down at the micellar surface compared to the bulk acetonitrile solution.

Keywords: Core-modified water-soluble porphyrins; Photoinduced electron transfer; Aggregation; Resonance light scattering (RLS); Micelle; Fluorescence quenching

1. Introduction

Water-soluble porphyrins have generated considerable interest in recent times [1,2], due to their applications as model systems for photosynthesis as well as their potential applications as second and third generation sensitizers for photodynamic therapy [3–6]. Core-modified porphyrins are especially attractive in this respect, as they have been found to be more effective as photosensitizers than the more widely studied sulphonated tetraphenyl porphyrin ($TPPS_4$), which absorb weakly in the therapeutic region (650–700 nm) and exhibit neurotoxicity [7], whereas the substitution of nitrogen with heteroatom such as S, O, Se, Te shifts the absorption bands towards longer wavelength. Furthermore the water-soluble porphyrins exhibit interesting aggregation properties and are likely to find applications in opto-electronic devices and non-linear optics as well [8–10]. Interestingly, except for one report by us, there are no reports on cationic water-soluble heteroporphyrins [11]. In this paper, we report the synthesis, characterization of a series of water-soluble 21-thiaporphyrins **6–8** and 21-oxaporphyrins **9–10** bearing three *N*-methylpyridinium ions at the *meso*-positions (Plate 1).

A second aspect of the present communication is the surfactant-induced aggregation/deaggregation of these porphyrins and Photoinduced Electron Transfer (PET) between selected porphyrins with neutral aromatic amines in bulk acetonitrile and SDS micellar media. The objective behind the study of PET in porphyrinic systems in organized media stems from the urge to develop efficient systems leading to the formation of long-lived ion pairs, so that the energy produced thus can be used fruitfully [12,13]. The first step towards development of such systems is to understand that the rate of electron transfer depends on the distance of donor and accepter moieties. If this distance is too large for the reactants to diffuse to each other during the excited state lifetimes, then PET is suppressed. On the other hand, if the distance is comparable to the van der Waals radius, that the back electron transfer is also ultrafast, leading

* Corresponding authors. Tel.: +91 22 2576 7149; fax: +91 22 2572 3480.
E-mail addresses: anindya@chem.iitb.ac.in (A. Datta), ravikanth@chem.iitb.ac.in (M. Ravikanth).

1010-6030/$ – see front matter © 2007 Elsevier B.V. All rights reserved.
doi:10.1016/j.jphotochem.2007.06.022

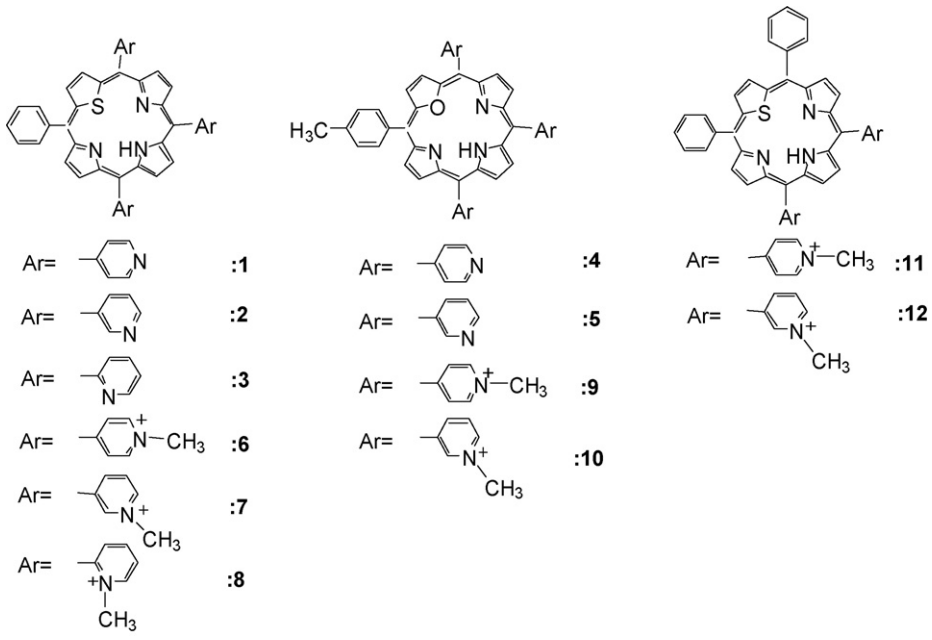

Plate 1.

to a very short-lived ion pair. The challenge, therefore, lies in the design of systems where this distance can be controlled in order to have an efficient forward electron transfer and a negligible back electron transfer. This goal can be achieved either by entrapment of the donor or acceptor in organized assemblies like micelles. This has prompted several attempts to develop donor–acceptor systems based on organized assemblies [14–16].

2. Results and discussion

2.1. Synthesis of meso-pyridyl 21-thia and 21-oxaporphyrins

To synthesize the cationic water-soluble porphyrins **6**–**10**, the 21-thia and 21-oxaporphyrins, having three pyridyl groups at the *meso*-positions **1**–**5** are required. These pyridyl porphyrins were synthesized by following the mono-ol methodology developed recently in our laboratory [17]. The mono-ols, 2-[α-phenyl-α-hydroxymethyl]thiophene and 2[α-tolyl-α-hydroxymethyl]furan were prepared in 65–70% yields by treating thiophene and furan, respectively, with 1.2 equivalents of *n*-butyl lithium followed by 1.2 equivalents of benzaldehyde or tolyl aldehyde in THF at 0 °C. The 21-thiaporphyrins **1**–**3** were prepared by condensing the two equivalents of 2-[α-phenyl-α-hydroxymethyl]thiophene with two equivalents pyridine-2, 3 or 4-carboxaldehyde and three equivalents of pyrrole in propionic acid at refluxing temperature for 2 h (Scheme 1). The propionic acid was removed under vacuum and the crude solid after thorough wash with warm water and drying at 100 °C was passed through silica gel column using CH_2Cl_2/CH_3OH to remove the non-porphyrinic impurities. The TLC analysis of the compound showed the formation of two porphyrins with two different porphyrin cores: *meso*-5,10,15,20-tetrapyridyl porphyrin (N_4 core) and the desired *meso*-5,10,15-tris(2, 3 or 4-pyridyl)-20-phenyl-21-thiaporphyrin (N_3S core). The mixture was separated by silica gel column chromatography. The desired 21-thiaporphyrin **1**–**3** was collected as first band using CH_2Cl_2/CH_3OH and afforded dark purple solids in 2–6% yields. Although the yields were moderate, the compounds could be prepared in sufficient quantity in one pot, the precursors being easily available. Furthermore, there is no other good strategy at present is available to prepare the trifunctionalized heteroporphyrins. The attempts to prepare the 21-thiaporphyrins **1**–**3** under $BF_3{\cdot}OEt_2$ or TFA conditions did not yield the porphyrin, suggesting the high refluxing conditions in propionic acid were compulsory to prepare these porphyrins.

The 21-monooxaporphyrins **4** and **5** were prepared similarly by condensing two equivalents of 2[α-tolyl-α-hydroxymethyl]furan with two equivalents of pyridine-3 or

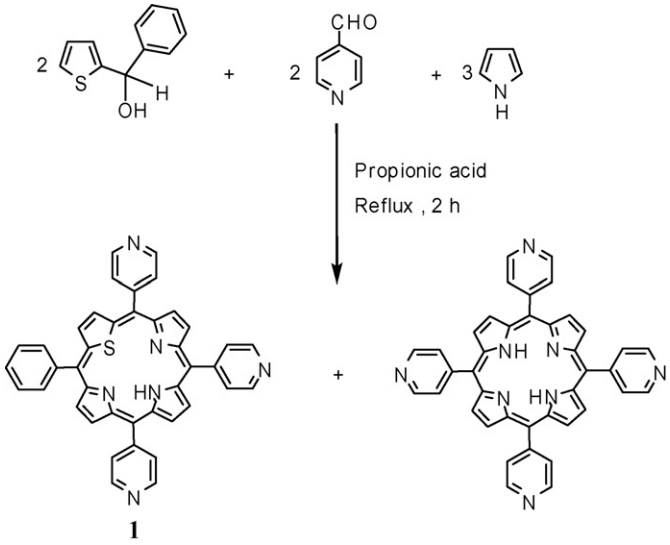

Scheme 1. Synthesis of 21-thiaporphyrin having three *meso*-4-pyridyl groups.

4-carboxaldehyde and three equivalents of pyrrole in propionic acid. The crude compound after column chromatography on silica showed the formation of two porphyrins: *meso*-5,10,15,20-tetrapyridylporphyrin (N_4 core) and the desired *meso*-5,10,15-tris(2, 3 or 4-pyridyl)-20-(*p*-tolyl)-21-oxaporphyrin (N_3O core). The mixture was separated by silica gel column chromatography and the desired 21-monooxaporphyrins **4** and **5** were collected as first band in 2 and 3% yields, respectively, as dark purple solids. The 21-oxaporphyrins **4** and **5** were formed in low yields and the purification by column chromatography was more cumbersome as compared to their 21-monothiaporphyrin analogs. Furthermore, the porphyrin did not form when we condensed 2[α-tolyl-α-hydroxymethyl]furan with pyridine-2-carboxaldehyde and pyrrole in refluxing propionic acid indicating the less reactivity of furan mono-ol.

The 21-thia- and 21-oxaporphyrins **1–5** were characterized by NMR, mass, absorption and elemental analysis. The unsymmetrical substitution of pyridyl porphyrins **1–5** was clearly evident in ^{1}H NMR which showed more number of peaks for thiophene/furan and pyrrole protons. The thiophene or furan which generally appears as singlet in 5,10,15,20-tetraphenyl-21-thiaporphyrin (STPPH) or 5,10,15,20-tetraphenyl-21-oxaporphyrin (OTPPH) [18] appeared as two signals in **1–5** indicating the low symmetric nature of the porphyrins. The M^+ ion peak in mass spectra and matching elemental analysis confirmed the composition of the porphyrins. The absorption spectra of **1–5** showed four typical Q-bands and one Soret band with peak maxima matching with STPPH or OTPPH [18]. The fluorescence spectra of **1–5** also showed two bands with identical peak maxima with that of STPPH or OTPPH [18].

2.2. Synthesis of cationic water-soluble 21-thia and 21-oxaporphyrins (*6–10*)

The cationic water-soluble 21-thia and 21-oxaporphyrins **6–10** were prepared by treating the porphyrin **1–5**, respectively, with 500-fold excess of CH_3I in CH_2Cl_2 at refluxing temperature for overnight (Scheme 2). The solid was formed on the walls of the round bottom flask as the reaction progressed and the dark brown solution became pale yellow colour. The compounds were filtered and washed several times with CH_2Cl_2. The compounds were recrystallized two times using CH_3OH/diethyl ether and afforded water-soluble porphyrins **6–10** in 45–50% yields. The porphyrins were highly soluble in water, CH_3OH, DMSO and DMF. The water-soluble porphyrins **6–10** were characterized by NMR, mass, absorption and elemental analysis. The porphyrins **6–10** showed high tendency to aggregate in water and methanol hence the ^{1}H NMR were recorded in $(CD_3)_2SO$ in which the porphyrins almost remain monomeric. ^{1}H NMR spectra of **6–10** showed more signals for thiophene/furan and pyrrole protons due to low symmetric nature of the porphyrins. The occurrence of the reaction was evident in the appearance of signal for pyridinium methyl group at 4.63 ppm (Fig. 1). The methylation of the pyridyl nitrogen resulted in a down field shift of the inner NH, pyridyl, β-thiophene/β-furan and β-pyrrole protons and maximum effects were observed for the pyridyl protons which were adjacent to the methylated nitrogen. For example, the inner NH and 2,6-pyridyl protons of **1** observed at −2.64 and 9.06 ppm, respectively, were shifted to −3.12 and 9.39 ppm in **6** indicating a change in the porphyrin ring current on methylation. The $[M-3I]^+$ion peaks in ES-MS mass spectra and matching elemental analysis confirmed the identity of the compounds **6–10**.

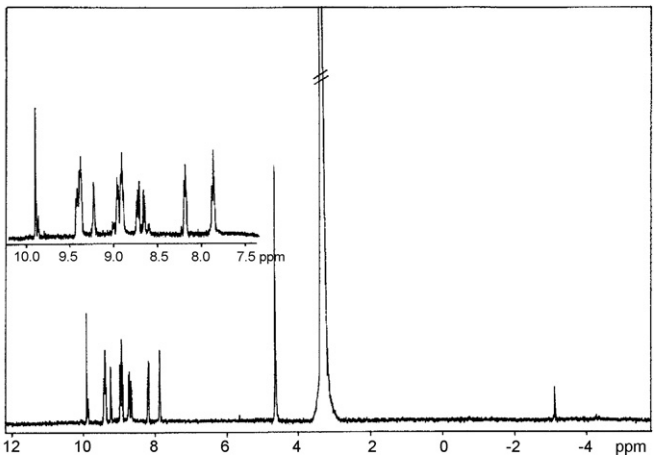

Fig. 1. ^{1}H NMR spectrum of **6** recorded in $(CD_3)_2SO$. The inset shows the expansion of 7.5–10.0 ppm region.

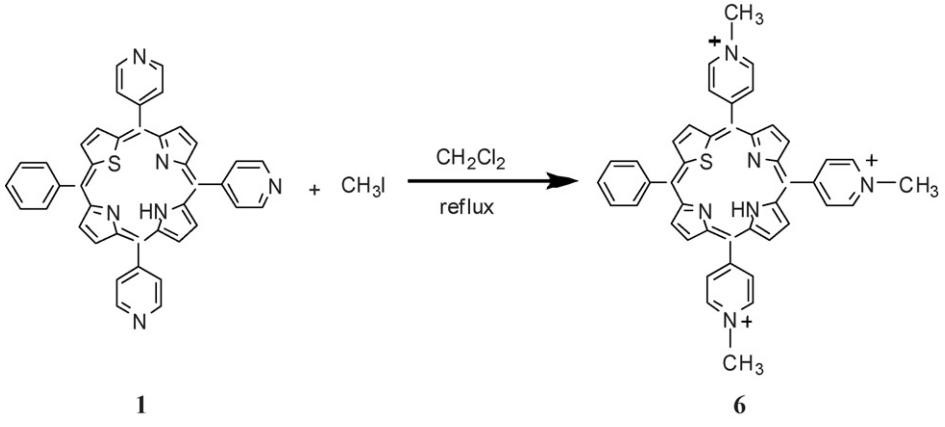

1 **6**

Scheme 2. Synthesis of water-soluble 21-thiaporphyrin having three *N*-methylpyridinium ions at the *meso*-positions.

2.3. Self aggregation in water

Water-soluble porphyrins have a high tendency for aggregation. Porphyrin aggregates have attracted much of interest because of their unique spectroscopic and electronic properties. These aggregates have potential applications in the field of photodynamic therapy, light harvesting system, molecular electronics, molecular biology applications, photoconductors, etc. [9,10,19]. The aggregation properties of selected water-soluble 21-thia and 21-oxaporphyrins have been investigated using absorption and emission spectroscopic studies. The water-soluble porphyrins **6–10** remain almost monomeric at low concentration in DMSO. Both 21-thia and 21-oxa water-soluble porphyrins **6–10** showed the typical structured Q-band and single Soret band in DMSO (Fig. 2A) [20]. The cationic 21-thiaporphyrins **6–8** followed Beer-Lambert's law in water in the concentration range 9×10^{-9} to 1.5×10^{-4} M and showed aggregation behaviour above 1.5×10^{-4} M [20]. Interestingly, unlike cationic 21-thiaporphyrins **6–8**, 21-oxaporphyrins **9** and **10** aggregate very strongly even at very low concentrations (10^{-6} to 10^{-7} M). The comparison of Q-band and Soret band absorption spectra of **9** in water and DMSO (2×10^{-6} M) is shown in Fig. 2B. It is very clear from Fig. 2B that the compound **9** in water showed only three Q-bands which are very broad and red shifted compared to the four Q-absorption bands of **9** in DMSO. Furthermore, the Soret band of cationic porphyrins **9** and **10** in water was very broad unlike in DMSO in which relatively narrow single Soret band was observed. The comparison of Q-band and Soret absorption spectra of cationic 21-thiaporphyrin **6** and cationic 21-oxaporphyrin **9** in water is shown in Fig. 3 at very low concentration (2×10^{-6} M). Unlike **6** which do not aggregate in water at this low concentration, the 21-oxaporphyrin **9** aggregates very strongly as reflected in its bathochromic structured Q-banded absorption spectra and broadened Soret band. Thus, the cationic 21-oxaporphyrins remain aggregated even at low concentration in water. The fluorescence studies were also in agreement with the absorption studies. The fluorescence spectra of **6–10** recorded in DMSO where the porphyrins remained monomeric showed a typical bimodal emission with peak positions typical of 21-thiaporphyrins and 21-oxaporphyrins. In water, at low concentration, the 21-thiaporphyrins, **6–8** remained monomeric (Fig. 4A) and emission maxima were identical with the emission maxima observed in DMSO. However, the 21-oxaporphyrins, **9–10** in water (Fig. 4A) were aggregated and emission maxima were bathochromically shifted as compared to the emission in DMSO (Table 1). The lifetimes of cationic 21-thiaporphyrins **6–8** in water were slightly shorter than that in DMSO (Table 1). However, for cationic 21-oxaporphyrin, **9–10**, the lifetime was decreased to ~3.5 ns from typical value of ~8.5 ns, supporting the aggregation of 21-oxaporphyrins (Fig. 4B). With this background, we now proceed to discuss the effect of surfactants on the aggregation behaviour of these cationic porphyrins, at concentrations where they do not undergo self-aggregation in water.

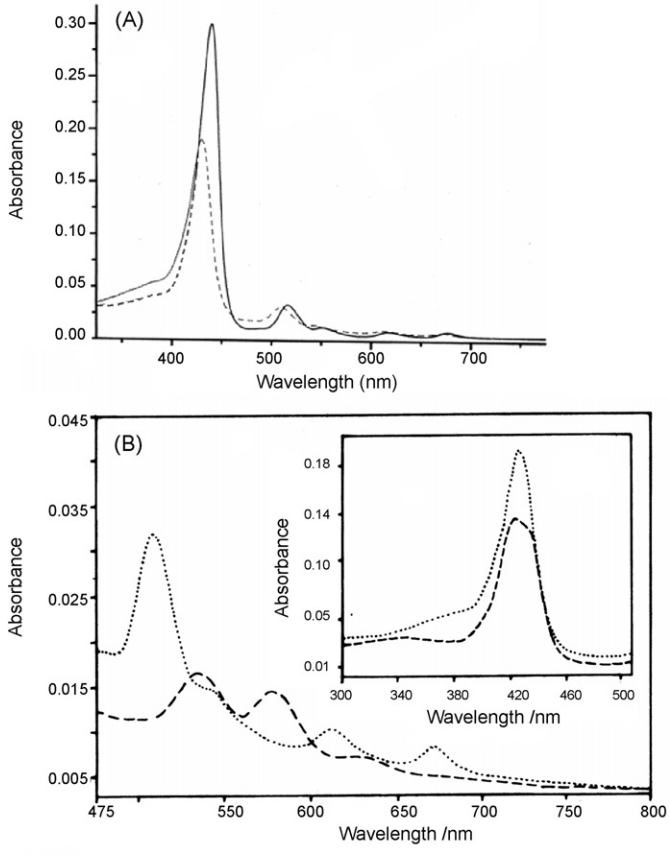

Fig. 2. (A) Comparison of absorption spectra of water-soluble porphyrins **6** (- - -) and **9** (—) in DMSO. (B) Q- and Soret (inset) band absorption spectra of **9** in water (- - -) and DMSO (· · ·). The concentration used was 2×10^{-6} M.

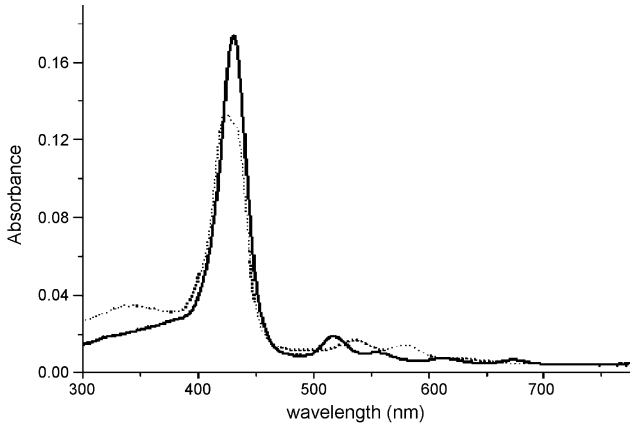

Fig. 3. Comparison of absorption spectra of 9 in water (- - -) and DMSO (· · ·). The concentration used was 2×10^{-6} M.

2.4. Surfactant induced aggregation and deaggregation

It is well known that surfactants can induce aggregation of porphyrins, often in a rather orderly fashion, below their CMCs. Beyond the CMC, the micelles are known to solubilize these aggregates [21–24]. We have performed steady state and time resolved spectroscopic investigations to study the aggregation of the cationic porphyrins at hand. Whereas the principal focus is on porphyrins **6** and **7**, the previously synthesized porphyrins **11** and **12** have also been studied in order to serve as a reference. The

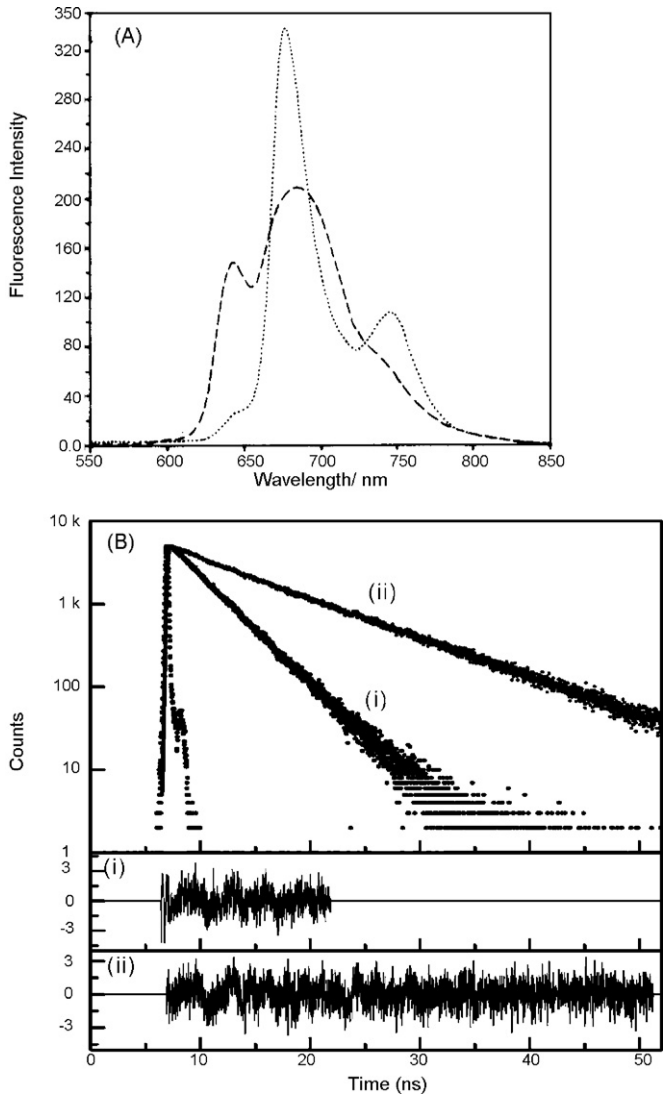

Fig. 4. (A) Fluorescence spectra of porphyrin **6** (···) and **9** (- - -) in water and (B) fluorescence decay curves of porphyrin **9** in (i) water and (ii) DMSO. The concentration used was 2×10^{-7} M.

absorption spectra of all the four cationic porphyrins were almost the same in aqueous solutions. The studies in micellar medium indicated that the remarkable spectral changes were induced by SDS in premicellar concentrations, but not by Triton X 100 or CTAB. This observation highlights the importance of the charge on the surfactant headgroup in surfactant-induced aggregation processes, as we have reported earlier [24]. On gradual addition of SDS from 0 to 0.2 mM, the Soret band at 425 nm exhibits a gradual red shift to 432 nm for **6** (Fig. 5A). Similar red shift has been observed from 428 to 432 nm for **7**, 424 to 432 nm for **11** and 428 to 432 nm for **12** on gradual increase of SDS concentration from 0 to 0.2 mM. The Q-bands are also shifted from 673 to 682 nm for all four porphyrins. These spectral shifts, accompanied by a decrease in absorbance, in the range of SDS concentration 0–0.2 mM indicate the formation of aggregates. The subsequent increase indicates the dissociation of surfactant induced aggregate at higher surfactant concentration (Fig. 5).

The steady state fluorescence data reinforce the contention derived from the UV–vis absorption experiments. For all the four porphyrins, addition of SDS causes a gradual decrease in the fluorescence quantum yield (ϕ_f) until a minimum is reached and on further addition of SDS, ϕ_f increases to saturation (Fig. 5B). This variation can be ascribed to the formation of aggregates at low concentrations of the surfactant, followed by their disruption and association with the micelles, above CMC. A peak shift of 4 nm is also observed in the fluorescence spectrum on

Table 1
Emission spectral data of *meso*-pyridyl 21-thiaporphyrins **1–3** and 21-oxaporphyrins **4–5** and their water-soluble derivatives **6–10**

Compound	Solvent	Emission peak maxima λ_{nm} (λ_{exc} = 430 nm)	τ (ns)
1	Toluene	680, 751	2.22
2	Toluene	683, 753	2.17
3	Toluene	680, 750	2.21
4	Toluene	676, 748	7.10
5	Toluene	675, 743	7.20
6	DMSO	683, 752	1.57
	H_2O	686, 758	2.07
7	DMSO	680, 748	1.80
	H_2O	681, 743	1.62
8	DMSO	678, 749	1.86
	H_2O	682, 747	1.38
9	DMSO	676, 746	8.38
	H_2O	696, 740	3.20
10	DMSO	675, 745	8.37
	H_2O	696, 741	2.88

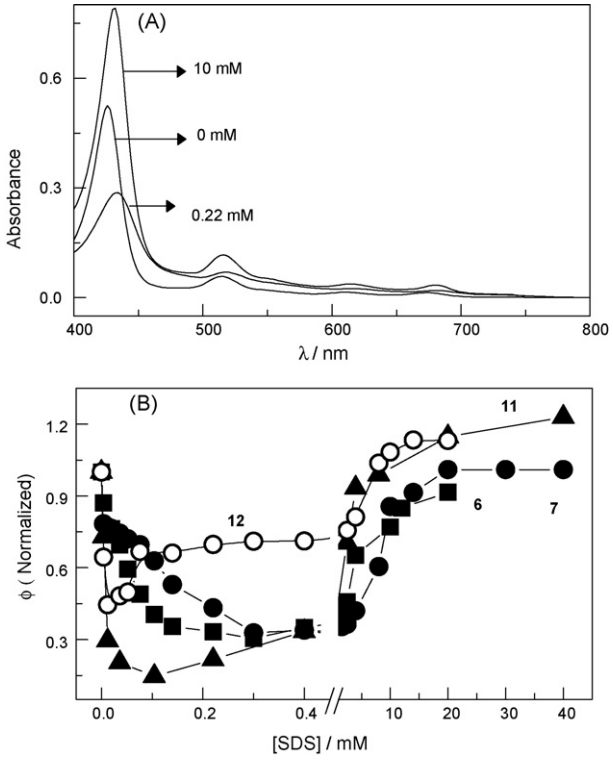

Fig. 5. (A) UV–vis spectra of porphyrin **6** at different concentrations of SDS and (B) variation of fluorescence quantum yield with concentration of SDS for porphyrin **6**,**7**, **11** and **12**.

Table 2
Variation of lifetime of porphyrins **6**, **7**, **11** and **12** with SDS concentration

[SDS] (mM)	Porphyrin **6** (τ/ns)	Porphyrin **7** (τ/ns)	Porphyrin **11** (τ/ns)	Porphyrin **12** (τ/ns)
0	2.07	1.62	1.35	1.69
0.004	1.93	1.55	1.22	1.67
0.020	0.90	1.45	1.14	1.56
0.036	0.33	1.20	0.50	1.33
0.076	0.19	0.95	0.48	1.18
0.104	0.16	0.66	0.48	1.14
0.140	0.17	0.55	0.49	1.14
0.220	0.19	0.65	0.51	1.15
0.400	0.24	0.71	0.52	1.16
0.800	0.24	1.11	0.60	1.24
1.60	0.28	1.28	0.67	1.35
2.50	0.38	1.39	0.84	1.42
4.00	0.68	1.56	0.88	1.51
6.00	1.99	1.67	1.01	1.60
8.00	2.62	1.70	1.40	1.66
12.0	2.79	1.70	1.50	1.76
20.0	3.10	1.72	1.55	1.87

increasing the concentration of SDS from 0 to 10 mM. The concentration at which the minimum in ϕ_f is attained follows a pattern. It increases as the charge on the porphyrin increases and shows very little dependence on the position of the charge (Table S2). This observation can be rationalized, keeping in mind that the minima in these plots denote the onset of formation of porphyrin monomers as a predominant process over surfactant induced aggregation. Porphyrins with a smaller charge require a smaller number of surfactant molecules to form the premicellar complexes and so, for them, the minimum point is attained at a smaller surfactant concentration.

From the time resolved fluorescence experiment, the lifetimes for porphyrins **6**, **7**, **11** and **12** in aqueous solutions have been found to be 2.07, 1.62, 1.35 and 1.69 ns, respectively (Table 2). The variations of lifetimes of all four porphyrins with addition of SDS are summarized in Table 2. For all the four porphyrin the lifetime initially decreases with increase in SDS concentration and again increases after reaching a minimum point to attain a saturation value. The decrease in lifetime follows the same pattern as in steady state fluorescence results. The saturation lifetimes of all the porphyrins are slightly higher than the lifetime of monomer porphyrins due to the micellization effect. These results are in line with the steady state data. The initial decrease in lifetime marks the formation of porphyrin aggregates and then the increase in lifetime is due to the disruption of these aggregates due to complexation with the SDS molecules and finally when the porphyrin molecules get associated with the SDS micelles a saturation of the radiative lifetime is attained.

The fluorescence results as described above, indicates the formation and subsequent disruption of aggregates. In order to monitor the formation of aggregates by a more direct method, we have performed the Resonance Light Scattering (RLS) experiment. It is observed as increased scattering intensity at or very near the wavelength of absorption of an aggregated molecular species. The effect is enhanced by several orders of magnitude when strong electronic coupling exists among the chromosomes

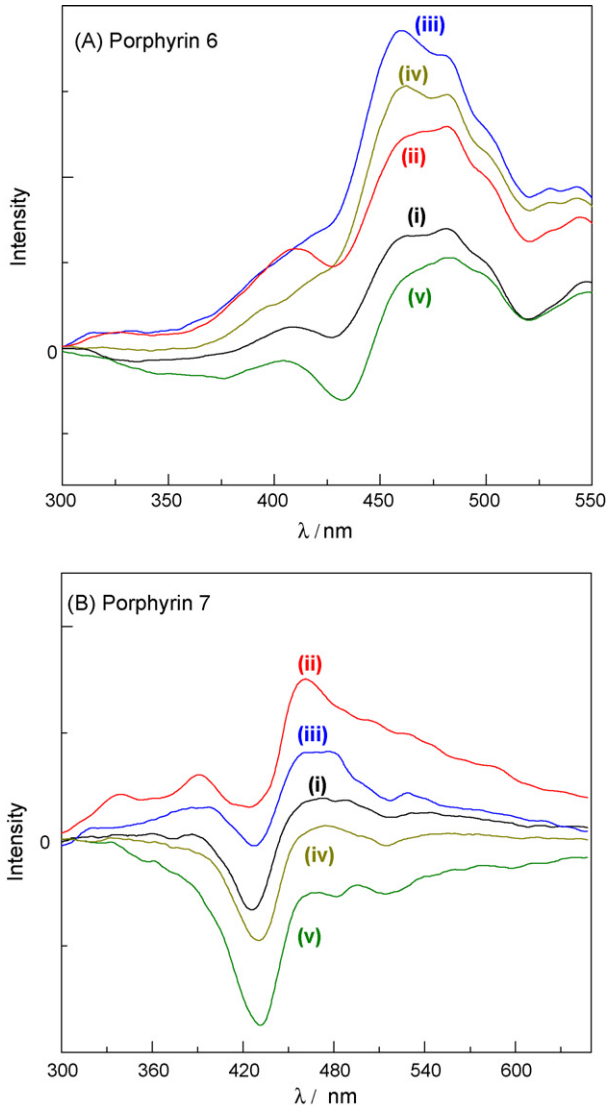

Fig. 6. RLS spectrum of (A) porphyrin **6** with (i) 0 mM, (ii) 0.005 mM, (iii) 0.05 mM, (iv) 0.25 mM, (v) 12 mM SDS and (B) porphyrin **7** with (i) 0 mM, (ii) 0.01 mM, (iii) 0.10 mM, (iv) 4 mM, (v) 12 mM SDS.

[25]. In the RLS monitoring of aggregates, the monomers are known to exhibit a dip or trough at the absorption maximum while aggregates exhibit a peak near maximum absorption wavelength indicating that the size of the aggregate is large enough to scatter light and there are multiple porphyrin molecules per aggregate. Thus, RLS has become an important tool for test of formation of aggregates [26]. The representative RLS spectra of porphyrin 6 and 7 at different SDS concentrations are shown in Fig. 6. It has been observed that in the absence of surfactants, the RLS spectrum of **6** comprises of a very small trough at 428 nm, coincident with the Soret absorption. This trough becomes less prominent and a peak is observed at 465 nm in the presence of 0.05 mM SDS. Above this concentration, the peak height at 465 nm decreases gradually and finally above CMC a trough at 432 nm is observed. The Same trend has been observed for porphyrin 7, where in absence of any surfactant a prominent trough at 426 nm has been observed. With subsequent addition of SDS a broad peak at 465 nm appears with a maximum quan-

tum yield at 0.01 mM SDS concentration has been observed. The aggregated peak at 465 nm vanishes completely at 12 mM SDS concentration with a large trough at 431 nm. This is a clear indication of initial formation of aggregates and subsequent disruption of these aggregates in the presence of micelles, as has been suggested in the absorption and fluorescence experiments.

2.5. Photoinduced electron transfer between cationic porphyrins (7 and 12) and aromatic amines in acetonitrile and SDS micelle

The steady state absorption spectra of porphyrin **7** and porphyrin **12** in water get red shifted (6 nm) from 428 to 434 nm in presence of 100 mM SDS [20], indicating ground state association between these cationic porphyrins and SDS micelles due to their opposite charges [23,24,27]. The fluorescence spectra of these two porphyrins are also red shifted by 5 nm with increase in quantum yield. The absorption spectra of both the porphyrins are unaffected by the addition of *N*,*N*-dimethylaniline (DMA) and aniline (AN), indicating no ground state association or complex formation. On the other hand, the fluorescence intensity of both the porphyrins get quenched by the amines in acetonitrile as well as in SDS micelles [20]. The spectral shape and peak position remain the same. The quenching of fluorescence may occur due to a number of photo-processes that can occur in the excited state, namely electron transfer, energy transfer, proton transfer, hydrogen bonding, etc. The possibility of energy transfer can be ruled out due to lack of spectral overlap between the donor and acceptor molecules. On the other hand, proton transfer and hydrogen bonding interaction is not possible in the present system due to unavailability of a labile proton. Hence the mechanism of quenching is only due to photoinduced electron transfer from aromatic amines to cationic porphyrins.

In the present system both the aromatic amines (DMA and AN) are insoluble in water but are quite soluble in presence of SDS micelles. From the previous study it is known that these amines reside exclusively on the Stern layer of SDS micelles [14,28]. From the steady state absorption and fluorescence data discussed earlier, it is quite clear that both the prophyrins are associated with the micelles, due to the interplay of electrostatic as well as hydrophobic interactions. Hence, the electron transfer occurs in the micellar surface. To have a quantitative estimation of the quenching process in the SDS micellar system, Steady state fluorescence quenching results were correlated using the Stern-Volmer (SV) relation,

$$\frac{\phi_0}{\phi} = 1 + K_{sv}[Q]_{eff} = 1 + k_q\tau_0[Q]_{eff}$$

where ϕ_0 and ϕ are the fluorescence quantum yields for the porphyrins in the absence and presence of the quenchers, respectively, K_{SV} the Stern-Volmer constant, k_q the bimolecular quenching rate constant, τ_0 the lifetime of the porphyrins in absence of quencher and $[Q]_{eff}$ is the effective concentration of the amine quenchers in the micellar Stern layer, estimated from the following consideration. The average diameter of SDS micelles is 60 Å, with a non-polar core diameter of 42 Å [29]. Hence the diameter of the Stern layer is about 18 Å. Thus, the

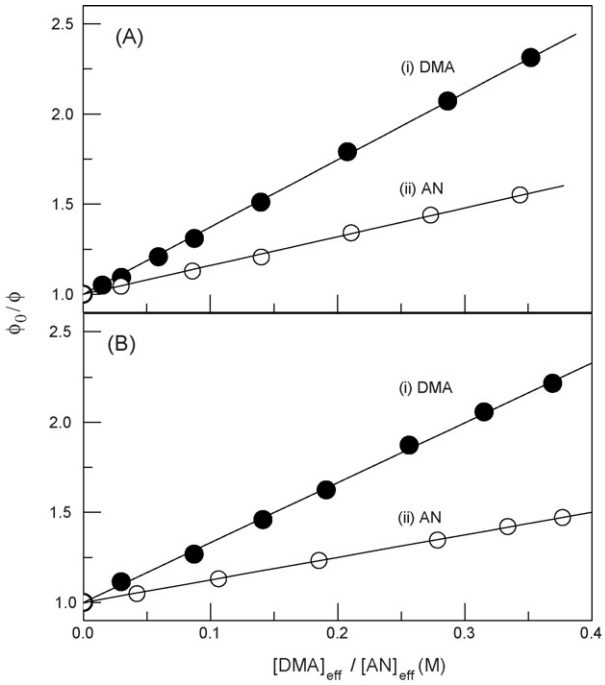

Fig. 7. Stern-Volmer plots using quantum yields for quenching of (A) porphyrin **7** and (B) porphyrin **12** by DMA and AN in 100 mM SDS.

volume of the micellar Stern layer is about 7.4×10^4 Å^3 per micelles or 44.75 dm^3 per mole of the micelle. Considering all the amine donors to reside in the Stern layer, the effective amine concentration is calculated by

$$[Q]_{eff} = \frac{N_{agg}[Q]_t}{44.75\{[SDS]_t - CMC\}}$$

where N_{agg} is the average aggregation number for SDS micelle ($N_{agg} = 62$) [28], $[SDS]_t$ the total SDS concentration used (100×10^{-3} mol dm^{-3}), CMC the critical micellar concentration of SDS (8×10^{-3} mol dm^{-3}) and $[Q]_t$ is the total amine concentration used in the system. The Stern Volmer plots are linear, suggesting that only one type of quenching mechanism is operative (Figs. 7 and 8). The slope of these plots yields the Stern-Volmer constant (K_{SV}) and the quenching rate constant k_q is calculated therefrom (Table 3). The extent of fluorescence quenching by DMA and AN is different for both the

Table 3
Correlation between steady state and time resolved quenching data for porphyrin **7** and **12** in 100 mM SDS

Porphyrin	Medium	τ_0 (ns)	Amines	k_q (10^9 M^{-1} s^{-1})	
				SS	TR
7	SDS	1.68	DMA	2.27	1.22
			AN	0.98	0.55
	CH_3CN	1.93	DMA	10.60	9.50
			AN	5.20	4.04
12	SDS	1.90	DMA	1.75	0.76
			AN	0.63	0.32
	CH_3CN	2.11	DMA	9.30	8.50
			AN	2.30	1.45

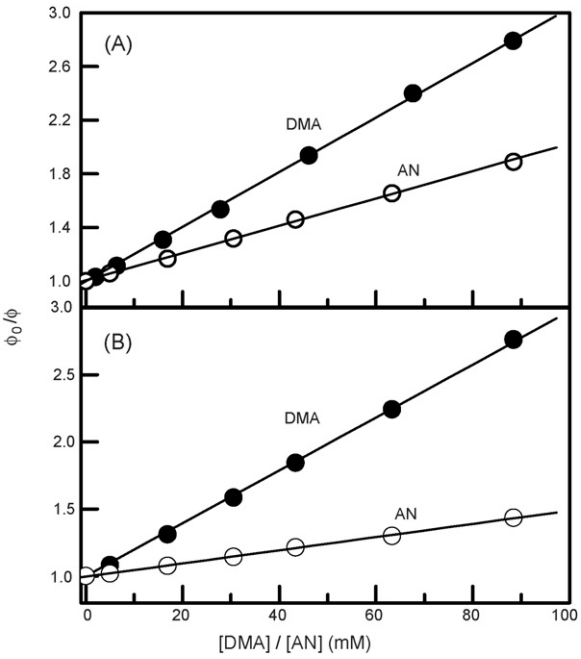

Fig. 8. Stern-Volmer plots using quantum yields for quenching of (A) porphyrin **7** and (B) porphyrin **12** by DMA and AN in acetonitrile.

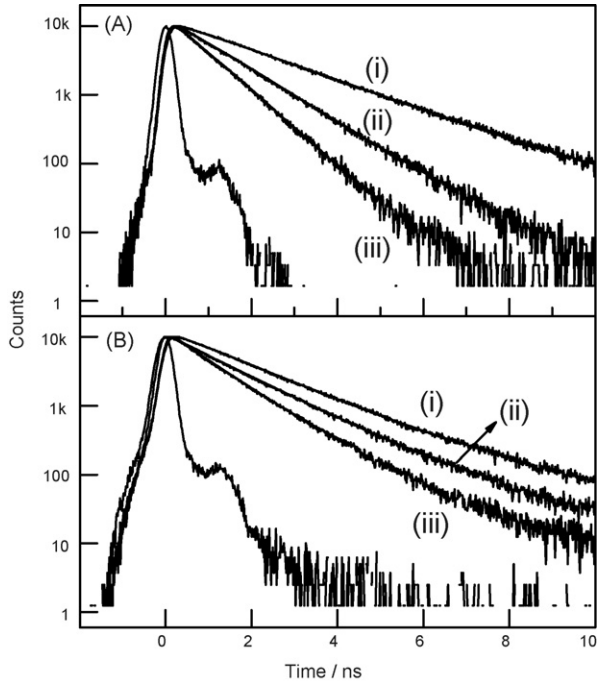

Fig. 9. Fluorescence decays of porphyrin **7** in (A) acetonitrile with (i) 0 mM, (ii) 43.36 mM (iii) 88.46 mM and (B) 100 mM SDS with (i) 0 mM, (ii) 9.30 mM, (iii) 27.8 mM of DMA.

porphyrins. The quenching efficiency of DMA is higher than that of AN (Table 3), which is expected due to their difference in redox potential [14,15]. Similarly porphyrin 7 gets more quenched than that of porphyrin 12 due to the higher positive charge and the consequent greater electron accepting ability of the first. The quenching rate of porphyrin 7 has a value of $2.27 \times 10^9\ M^{-1}\ s^{-1}$ in presence of DMA whereas it has a value of $1.75 \times 10^9\ M^{-1}\ s^{-1}$ for porphyrin 12. Here it is worthwhile to compare the present results with the previously obtained results of chlorin p_6 with methyl viologen [16]. The quenching rate (k_q) in that case was much higher ($7.4 \times 10^{12}\ M^{-1}\ s^{-1}$ in presence of 20 mM SDS). This is rationalized by the opposite charges on the two reactants chosen, which would cause a reduced effective encounter distance and consequently, a greater coupling strength between donor and accepter molecules, in accordance with Marcus theory [30,31]. Thus, we find that the rate of PET in micellar media is governed by an interplay of hydrophobic and electrostatic effects. In order to highlight another important point in this regard, we have studied the electron transfer in bulk acetonitrile as well, where the electron transfer rate is much faster than in micelles (Figs. 7 and 8; Table 3). This observation is rationalized in the light of a greater microviscosity inside the micelle, leading to an increased effective encounter distance between the porphyrins and amines due to the intervention of the hydrophobic surfactant chain [14,15].

To obtain a better understanding of the dynamics of the fluorescence quenching time resolved fluorescence experiment has been performed. The fluorescence lifetimes of both the porphyrin decrease with gradual addition of amines in acetonitrile and SDS micelles (Fig. 9). In acetonitrile, all the decays are single exponential. In presence of 100 mM SDS, **7** has a lifetime of 1.68 ns, which decreases to 0.90 ns at 27.8 mM of DMA. Similarly, the lifetime of **12**, which is 1.90 ns at 100 mM SDS,

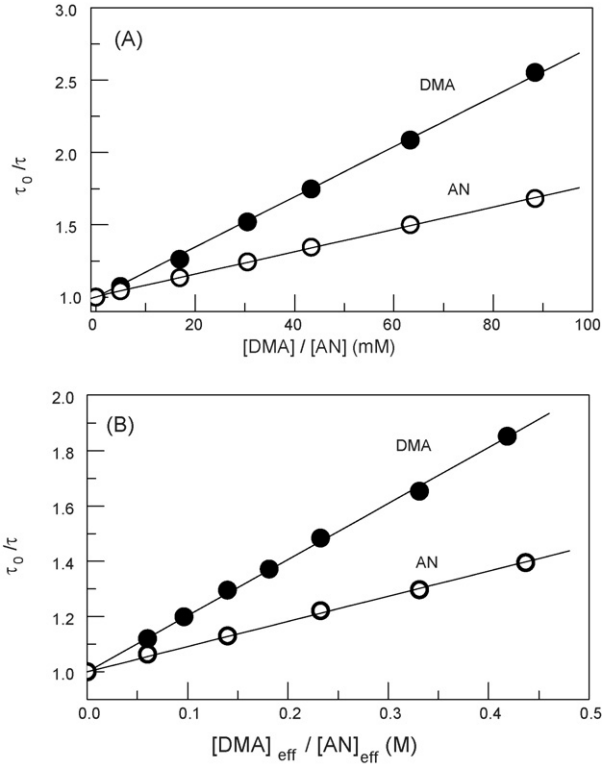

Fig. 10. Stern-Volmer plots using fluorescence lifetimes for quenching of porphyrin **7** in (A) acetonitrile and (B) 100 mM SDS by DMA and AN.

decreases to 1.18 ns in the presence of 28 mM of DMA. Similar results have been observed in the presence of aniline donor, but the extent of quenching is lesser (Table 3). The corresponding quenching constant is determined from the following equation:

$$\frac{\tau_0}{\tau} = 1 + K_{SV}[Q]_{eff}$$

The plot of τ_0/τ versus $[Q]_{eff}$ is shown in Fig. 10. In neat acetonitrile solution the time resolved data are well correlated with the steady state measurement (Table 3). The somewhat larger value of k_q obtained in steady state measurement in SDS micelles, as has been observed in earlier reports as well [14,16]. The plausible explanation may be that, in some micelle the amines and the porphyrin trapped very close to each other and some part of the ET rate in the micelle is expected to be almost ultrafast. This hypothesis gets support from the recent femtosecond study of PET between coumarin accepter and amine donors in micellar system by Bhattacharyya and co-workers. They have observed that even in micellar medium the quenching rate has an ultrafast component, which has a value of <10 ps [32].

3. Conclusion

A series of cationic water-soluble 21-thia and 21-oxaporphyrins were synthesized by methylating the appropriate *meso*-pyridyl 21-thia and 21-oxaporphyrins with methyl iodide in toluene. A preliminary aggregation properties studied for selected cationic water-soluble porphyrins having three *N*-methylpyridinium groups at *meso*-positions indicated that the cationic water-soluble 21-oxaporphyrins have very high tendency to aggregate as compared to cationic water-soluble 21-thiaporphyrins. The negatively charged surfactant, sodium dodecyl sulfates, was found to induce aggregation of the water-soluble cationic 21-thiaporphyrins at submicellar concentrations. The premicellar aggregation is found to be governed by the electrostatic attraction between the cationic 21-thiaporphyrins and oppositely charged surfactant molecules. These aggregates were found to be solubilized in micelles found at higher surfactant concentration. In such micellar concentration, it was possible to bring about the photoinduced electron transfer reaction between the cationic porphyrins and neutral aromatic amines, which is not possible in aqueous solution. It has been observed that the electron transfer rates become slower in micellar medium as compared to the bulk acetonitrile solution due to the higher microviscosity at the micellar surface.

4. Experimental

4.1. General

Aniline (AN) and *N*,*N*-dimethylaniline (DMA) were obtained from Spectrochem (India) and purified by vacuum distillation just before use. Sodium dodecyl sulfate (SDS) from Aldrich have been used as received. The concentration of the porphyrins used is 4×10^{-6} M. All the aqueous solutions have been prepared in doubly distilled water. The absorption and fluorescence spectra were recorded on JASCO V570 spectrophotometer with 2 nm band pass and on a Perkin-Elmer LS-55 spectrofluorimeter, respectively. Fluorescence decays were measured using the time correlated single photon counting (TCSPC) spectrometer setup from IBH, with a 250 ps pulse from a solid state diode laser, emitting at 406 nm. The fluorescence decays were collected at 680 nm. All measurement was done taking the emission polarizer at magic angle 55.4°. The decays were analysed by the iterative deconvolution method using the IBH DAS 6.0 software.

4.2. 5,10,15-Tris(4-pyridyl)-20-phenyl-21-monothiaporphyrin building block (1)

Samples of 2-(α-tolyl-α-hydroxymethyl)thiophene (500 mg, 2.63 mmol), pyridine-4-carboxaldehyde (249 μL, 2.63 mmol) and pyrrole (273 μL, 3.95 mmol) in 75 mL of propionic acid was refluxed for 3 h. The reaction mixture was left for overnight at room temperature. The propionic acid was removed under reduced pressure. The black residue thus obtained was washed several times with warm water and kept in oven at 100 °C for 10 min. The dark crude product of mixture of two porphyrins along with non-porphyrinic impurities was then dissolved in minimum amount of CH_2Cl_2 and dry slurry powder was prepared by adding silica gel and removed the traces of solvent under vacuum. Column chromatography on silica using CH_2Cl_2/4%CH_3OH followed by recrystallization with CH_2Cl_2/petroleum ether gave **1** as purple solid in 6% yield (91 mg). mp > 300 °C. IR (KBr, ν cm^{-1}) 3434, 2861, 2400, 1591. ^{1}H NMR (300 MHz, $CDCl_3$, δ in ppm) −2.84 (s, 1H, NH), 7.84 (m, 3H, Ar), 8.16 (m, 4H, 3, 5-pyridyl and Ar), 8.20 (m, 2H, 3, 5-pyridyl), 8.24 (m, 2H, 3, 5-pyridyl), 8.57 (d, J = 4.7 Hz, 1H, β-pyrrole), 8.61 (d, J = 4.7 Hz, 1H, β-pyrrole), 8.70 (d, J = 4.6 Hz, 1H, β-pyrrole), 8.76 (d, J = 4.4 Hz, 1H, β-pyrrole), 8.94 (d, J = 1.9 Hz, 2H, β-pyrrole), 9.05 (m, 4H, 2,6-pyridyl), 9.09 (m, 2H, 2, 6-pyridyl), 9.73 (d, J = 5.5 Hz, 1H, β-thiophene), 9.85 (d, J = 5.5 Hz, 1H, β-thiophene). ^{13}C NMR (100 MHz, $CDCl_3$): δ 21.5, 29.7, 126.9, 127.4, 128.3, 128.5, 128.9, 130.7, 131.7, 132.6, 132.8, 133.1, 133.6, 134.2, 134.4, 134.6, 135.5, 135.7, 137.6, 138.0, 139.1, 139.5, 141.8, 146.9, 148.3, 154.6, 156.8, 157.6. ES-MS: $C_{41}H_{26}N_6S$, calcd. av. mass, 634.7, obsd. m/z 635.4 (M^+). Anal. calcd.: C, 77.58; H, 4.13; N, 13.24; S, 5.05. Found: C, 77.18; H, 4.10; N, 13.32; S, 5.19.

4.3. 5,10, 15-Tris (3-pyridyl)-20-phenyl-21-monothiaporphyrin building block (2)

A solution of 2-(α-tolyl-α-hydroxymethyl)thiophene (500 mg, 2.63 mmol), pyridine-3-carboxaldehyde (249 μL, 2.63 mmol) and pyrrole (273 μL, 3.95 mmol) were dissolved in 75 mL of propionic acid and refluxed for 3 h. The reaction mixture was worked up as mentioned for **1**. The mixture of two porphyrins was separated by silica gel column chromatography and the desired compound **2** was obtained using CH_2Cl_2/4%CH_3OH. Recrystallization with CH_2Cl_2/petroleum

ether gave pure **2** as purple solid (79 mg, 5%). mp > 300 °C. IR (KBr, ν cm^{-1}) 3421 (NH), 2934, 2861, 802, 696. ^{1}H NMR (400 MHz, $CDCl_3$, δ in ppm) −2.74 (s, 1H, NH), 7.79 (m, 7H, 4, 5-pyridyl and Ar), 8.24 (br, s, 2H, 4, 5-pyridyl), 8.53 (m, 3H, 4, 5-pyridyl and β-pyrrole), 8.60 (d, J = 4.4 Hz, 1H, β-pyrrole), 8.69 (d, J = 4.4 Hz, 1H, β-pyrrole), 8.76 (d, J = 4.4 Hz, 1H, β-pyrrole), 8.94 (s, 2H, β-pyrrole), 9.04 (br s, 3H, 2, 6-pyridyl), 9.44 (m, 3H, 2, 6-pyridyl), 9.72 (d, J = 5.2 Hz, 1H, β-thiophene), 9.83 (d, J = 5.2 Hz, 1H, βthiophene). ^{13}C NMR (100 MHz, $CDCl_3$): δ 29.7, 119.6, 119.8, 121.9, 122.8, 127.5, 127.7, 128.2, 128.8, 128.9, 132.8, 133.3, 134.1, 134.2, 135.2, 135.5, 135.6, 136.6, 138.0, 138.7, 138.9, 140.4, 140.8, 147.6, 147.8, 149.3, 153.4, 154.5, 157.2, 157.9. ES-MS: $C_{41}H_{26}N_6S$, calcd. av. mass 634.7, obsd. *m/z* 635.1 (M^+). Anal. calcd.: C, 77.58; H, 4.13; N, 13.24; S, 5.05. Found: C, 77.83; H, 4.19; N, 13.21; S, 5.17.

4.4. 5,10,15-Tris (2-pyridyl)-20-phenyl-21-monothiaporphyrin building block (3)

A solution of 2-(α-tolyl-α-hydroxymethyl)thiophene (500 mg, 2.63 mmol), pyridine-2-carboxaldehyde (249 μL, 2.63 mmol) and pyrrole (273 μL, 3.95 mmol) were dissolved in 75 mL of propionic acid and refluxed for 3 h. After standard work-up, the crude porphyrin was subjected to silica gel column chromatography and the desired porphyrin **3** was collected using CH_2Cl_2/4%CH_3OH. The solvent was removed on rotary evaporator to afford **3** as a pure purple solid in 3% yield (49 mg). mp > 300 °C. IR (KBr, ν cm^{-1}): 3420, 2854, 2381, 1413, 1584, 1689, 702. ^{1}H NMR (400 MHz, $CDCl_3$, δ in ppm) −2.84 (s, 1H, NH), 7.65–7.79 (m, 8H, 4,5-pyridyls and Ar), 8.10–8.27 (m, 6H, 3-pyridyl and 4,5-pyridyls), 8.56 (br s, 2H, β-pyrrole), 8.73 (br s, 2H, β-pyrrole), 8.94 (s, 2H, β-pyrrole), 9.12 (br s, 2H, 6-pyridyl), 9.20 (br s, 1H, 6-pyridyl), 9.81 (br s, 1H, β-thiophene), 9.86 (br s, 1H, β-thiophene). ^{13}C NMR (100 MHz, $CDCl_3$, δ in ppm) 29.8, 121.3, 122.9, 127.7, 128.6, 130.5, 133.6, 134.5, 135.05, 135.9, 137.6, 144.4, 148.5, 151.8, 154.3, 168.4. ES-MS: $C_{41}H_{26}N_6S$, calcd. av. mass 634.7, obsd. *m/z* 635 (M^+). Anal. calcd.: C, 77.58; H, 4.13; N, 13.24; S, 5.05. Found: C, 77.83; H, 4.19; N, 13.21; S, 5.17.

4.5. 5,10,15-Tris (4-pyridyl)-20-(p-tolyl)-21-mono oxaporphyrin building block (4)

Samples of 2-(α-tolyl-α-hydroxymethyl)furan (500 mg, 2.64 mmol), pyridine-4-carboxaldehyde (248 μL, 2.64 mmol) and pyrrole (289 μL, 3.96 mmol) were dissolved in 75 mL of propionic acid and refluxed for 3 h. The reaction mixture was worked up as mentioned above and the crude compound was purified by silica gel column chromatography. The desired compound **4** was obtained as first band using CH_2Cl_2/4%CH_3OH and recrystallized with CH_2Cl_2/petroleum ether to afford pure **4** as purple solid in 3% yield (49 mg). mp > 300 °C. IR (KBr film, λ in cm^{-1}) 3414 (NH), 3046, 2927, 2855, 1591, 1472, 1407, 808, 736. ^{1}H NMR (400 MHz, $CDCl_3$, δ in ppm) 2.72 (s, 3H, CH_3), 7.59 (d, J = 7.6 Hz, 2H, Ar), 8.12 (m, 8H, 3, 5-pyridyl and Ar), 8.58 (m, 2H, β-pyrrole), 8.65 (m, 2H, β-pyrrole), 8.84 (m, 2H, β-pyrrole), 9.04 (m, 6H, 2,6- pyridyl), 9.19 (br s, 1H, β-furan), 9.34 (br s, 1H, β-furan). ^{13}C NMR (100 MHz, $CDCl_3$): δ 14.1, 21.6, 22.7, 31.9, 52.9, 70.6, 119.0, 120.0, 121.2, 122.2, 127.9, 129.1, 129.3, 129.8, 134.32, 134.7, 136.3, 138.4, 148.3, 148.7, 149.6, 150.3, 150.6, 154.0, 155.3. ES-MS: $C_{42}H_{28}N_6O$, calcd. av. mass 632.7, obsd. *m/z* 633.2 (M^+). Anal. calcd.: C, 79.73; H, 4.46; N, 13.28. Found: C, 79.93; H, 4.57; N, 13.39.

4.6. 5,10,15-Tris (3-pyridyl)-20-(p-tolyl)-21-mono oxaporphyrin building block (5)

A solution of 2-(α-tolyl-α-hydroxymethyl)furan (500 mg, 2.64 mmol), pyridine-3-carboxaldehyde (248 μL, 2.64 mmol) and pyrrole (289 μL, 3.96 mmol) in 75 mL of propionic acid was refluxed for 3 h and crude compound obtained was purified by silica gel column chromatography. The desired porphyrin **5** was collected using CH_2Cl_2/4%CH_3OH and recrystallized with CH_2Cl_2/petroleum ether to afford **5** as dark purple compound (32 mg, 2%). mp > 300 °C. IR (KBr, ν (cm^{-1})) 3401, 2935, 2374, 1413, 1466, 1584. ^{1}H NMR (400 MHz, $CDCl_3$, δ in ppm) 2.75 (s, 3H, CH_3), 7.71 (m, 2H, Ar), 7.87 (m, 2H, Ar), 8.39 (br s, 2H, 4,5-pyridyl), 8.70 (m, 9H, 4,5-pyridyl and β-pyrrole), 9.08 (m, 4H, β-pyrrole and 2-pyridyl), 9.38 (m, 1H, 6-pyridyl), 9.54 (m, 4H, 6-pyridyl and β-furan). ^{13}C NMR (100 MHz, $CDCl_3$, δ in ppm) 21.7, 27.4, 29.8, 31.9, 123.3, 129.4, 133.6, 136.5, 137.6, 149.8, 153.28. ES-MS: $C_{42}H_{28}N_6OI$, calcd. av. mass 632.7, obsd. *m/z* 633.1. Anal. calcd.: C, 79.73; H, 4.46; N, 13.28. Found: C, 79.62; H, 4.39; N, 13.15.

4.7. 5,10,15-Tris (4-N-methylpyridyl)-20-phenyl-21-thiaporphyrin (6)

Samples of **1** (100 mg, 0.1575 mmol) and 500-fold excess of CH_3I (4.90 mL, 78.769 mmol) in CH_2Cl_2 was refluxed for overnight. The compound was purified by recrystallization from methanol/diethyl ether and afforded crystalline purple solid (46 mg, 43%). mp > 250 °C. IR (KBr, ν cm^{-1}). 3414, 2947, 2381, 1453, 1637, 702. ^{1}H NMR (400 MHz, $CDCl_3$, δ in ppm). −3.12 (s, 1H, NH), 4.63 (s, 9H, NCH_3), 7.87 (m, 3H, Ar), 8.19 (m, 2H, Ar), 8.65 (m, 1H, 3,5-pyridyl), 8.73 (m, 3H, 3,5-pyridyl), 8.82 (m, 1H, 3,5-pyridyl), 8.95 (m, 6H, 3,5-pyridyl and β-pyrrole), 9.23 (br s, 1H, β-pyrrole), 9.39 (m, 6H, 2,6-pyridyl), 9.88 (m, 2H, β-thiophene). ES-MS: $C_{44}H_{35}N_6SI_3$, calcd. av. mass 1060.6, obsd. *m/z* 679.2. ($M-3I^-$). Anal. Calcd: C, 49.83; H, 3.33; N, 7.92; S, 3.02. Found: C, 51.05; H, 3.45; N, 8.13; S, 3.19.

4.8. 5,10,15-Tris (3-N-methylpyridyl)-20-phenyl-21-thiaporphyrin (7)

Compound **2** (100 mg, 0.1575 mmol) and 500-fold excess of CH_3I (4.90 mL, 78.769 mmol) in CH_2Cl_2 was refluxed for overnight. Recrystallization with methanol/diethyl ether gave 7 as purple solid (42 mg, 39%). mp > 250 °C. IR (KBr, ν cm^{-1}) 3427, 2933, 2361, 1459, 1650. ^{1}H NMR (400 MHz, $CDCl_3$, δ in

ppm). −3.07 (s, 1H, NH), 4.67 (s, 9H, NCH_3), 7.95 (m, 3H, Ar), 8.34 (m, 2H, Ar), 8.62 (m, 3H, 4,5-pyridyl), 8.81 (m, 3H, 4,5-pyridyl). 8.98 (br s, 1H, β-pyrrole), 9.36 (m, 5H, β-pyrrole), 9.52 (br s,3H, 2,6-pyridyl), 10.01 (m, 5H, 2,6-pyridyl and β-thiophene). ES-MS: $C_{44}H_{35}N_6SI_3$, calcd. av. mass 1060.6, obsd. *m/z* 679.4. ($M-3I^-$). Anal. Calcd: C, 49.83; H, 3.33; N, 7.92; S, 3.02. Found: C, 50.7; H, 3.42; N, 8.11; S, 3.11.

4.9. 5,10,15-Tris (2-N-methylpyridyl)-20-phenyl-21-thiaporphyrin (8)

Porphyrin **3** (100 mg, 0.1575 mmol) was dissolved in CH_2Cl_2 and 500-fold excess of CH_3I (4.90 mL, 78.769 mmol) was injected into the solution. The reaction mixture was refluxed for overnight. Recrystallization with methanol/diethyl ether afforded **8** as crystalline purple solid (40 mg, 37%). mp > 250 °C. IR (KBr, ν cm^{-1}) 3447, 2927, 2374, 1472, 1518, 1637, 748. ^1H NMR (400 MHz, $CDCl_3$, δ in ppm). −3.01 (s, 1H, NH), 5.74 (s, 9H, NCH_3), 7.89–7.99 (m, 5H, Ar), 8.28 (m, 3H, 4,5-pyridyls), 8.52 (m, 1H, 4,5-pyridyl), 8.72 (m, 4H, 4,5-pyridyl and 3-pyridyl), 8.81–8.98 (m, 8H, β-pyrrole and 3-pyridyl), 9.39 (m, 1H, 6-pyridyl), 9.65 (m, 2H, 6-pyridyl), 9.99 (s, 2H, β-thiophene). ES-MS: $C_{44}H_{35}N_6SI_3$, calcd. av. mass 1060.6, obsd. *m/z* 679.1. ($M-3I^-$). Anal. Calcd: C, 49.83; H, 3.33; N, 7.92; S, 3.02. Found: C, 50.11; H, 3.29; N, 8.01; S, 3.12.

4.10. 5,10,15-Tris (4-N-methylpyridyl)-20-(p-tolyl)-21-oxaporphyrin (9)

Samples of **4** (100 mg, 0.1575 mmol) and 500-fold excess of CH_3I (4.90 mL, 78.769 mmol) in CH_2Cl_2 was refluxed for overnight. The compound was recrystallized with methanol/diethyl ether and afforded pure **9** as a purple solid (42 mg, 39%). mp > 250 °C. IR (KBr, ν cm^{-1}): 3440, 2933, 2381, 1466, 1634. ^1H NMR (400 MHz, $CDCl_3$, δ in ppm). 3.16 (s, 3H, CH_3), 5.75 (m, 9H, NCH_3), 7.69 (d, $J = 8$ Hz, 2H, Ar), 8.12 (d, $J = 7.2$ Hz, 2H, Ar), 8.63 (d, $J = 4.8$ Hz, 1H, β-pyrrole), 8.68 (m, 1H, β-pyrrole), 8.73 (m, 1H, β-pyrrole), 8.77 (m, 1H, β-pyrrole), 8.98 (m, 6H, 3,5-pyridyls), 9.25 (s, 2H, β-pyrrole), 9.46 (br s, 6H, 2,6-pyridyls), 9.56 (d, $J = 4$ Hz, β-furan), 9.62 (d, $J = 5.6$ Hz, β-furan). ES-MS: $C_{45}H_{37}N_6OI_3$, calcd. av. mass 1058.5, obsd. *m/z* 677.1 $(M-3I^-)^+$. Anal. Calcd: C, 51.06; H, 3.52; N, 7.94. Found: C, 51.19; H, 3.51; N, 7.86.

4.11. 5,10,15-Tris (3-N-methylpyridyl)-20-(p-tolyl)-21-oxaporphyrin (10)

A solution of **5** (100 mg, 0.157 mmol) and 500-fold excess of CH_3I (4.90 mL, 78.76 mmol) in CH_2Cl_2 was refluxed for overnight. The compound was recrystallized from methanol/diethyl ether and obtained **10** as a crystalline purple solid (30 mg, 28%). mp > 250 °C. IR (KBr, ν cm^{-1}) 3447, 2903, 2369, 1465, 1634. ^1H NMR (400 MHz, $CDCl_3$, δ in ppm). 2.73 (s, 3H, CH_3), 4.64 (s, 9H, NCH_3), 7.74 (m, 1H, Ar), 8.15 (m, 3H, Ar), 8.54 (m, 2H, 4, 5-pyridyl), 8.77–8.99 (m, 6H, β-pyrrole and 4, 5-pyridyl), 9.04–9.39 (m, 9H, β-furan, β-pyrrole and 2-pyridyl), 9.95 (m, 3H, 6-pyridyl). ES-MS: $C_{45}H_{37}N_6OI_3$, calcd. av. mass 1058.5, obsd. *m/z* 677.3 ($M-3I^-$). Anal. Calcd: C, 51.06; H, 3.52; N, 7.94. Found: C, 52.10; H, 3.61; N, 8.09.

Acknowledgements

M.R. thanks DST and DAE, Govt. of India for financial support. A.D. thanks CSIR for a research grant. T.K.M. thanks UGC for a research fellowship.

Appendix A. Supplementary data

Supplementary data associated with this article can be found, in the online version, at doi:10.1016/j.jphotochem.2007.06.022.

References

[1] T.J. Dougherty, C.J. Gomer, B.W. Henderson, G. Jori, D. Kessel, M. Korbelik, J. Moan, Q. Peng, J. Natl. Cancer Inst. 90 (1998) 889–905.
[2] B.W. Henderson, T.J. Dougherty, Photochem. Photobiol. 55 (1992) 145–157.
[3] K.T. Moesta, P. Schlag, H.O. Douglass Jr., T.S. Mang, Lasers Surg. Med. 16 (1995) 84–92.
[4] T.J. Dougherty, S.L. Marcus, Eur. J. Cancer 28A (1992) 1734–1742.
[5] K. Berg, K. Prydz, J. Moan, Biochim. Biophys. Acta 1158 (1993) 300–306.
[6] D. Kessel, K. Woodburn, Int. J. Biochem. 25 (1993) 1377–1383.
[7] D.G. Hilmey, M. Abe, M.I. Nelen, C.E. Stilts, G.A. Baker, S.N. Baker, F.E. Bright, S.R. Davies, S.O. Gollnick, A.R. Oseroff, S.L. Gibson, R. Hilf, M.R. Detty, J. Med. Chem. 45 (2002) 449–461.
[8] T.J. Dougherty, Adv. Photochem. 17 (1992) 275–311.
[9] Y. Wang, Chem. Phys. Lett. 126 (1986) 209–214.
[10] F.C. Spano, S. Mukamel, Phys. Rev. 40A (1989) 5783–5801.
[11] S. Santra, D. Kumaresan, N. Agarwal, M. Ravikanth, Tetrahedron 59 (2003) 2353–2362.
[12] J. Jasieniak, M. Johnston, E.R. Waclawik, J. Phys. Chem. B 108 (2004) 12962–12971.
[13] J. Bisquert, D. Cahen, G. Hodes, S. Ruehle, A. Zaban, J. Phys. Chem. B 108 (2004) 8106–8118.
[14] M. Kumbhakar, S. Nath, H. Pal, A.V. Sapre, T. Mukherjee, J. Chem. Phys. 119 (2003) 388–399.
[15] A. Chakraborty, D. Chakraborty, P. Hazra, D. Seth, N. Sarkar, Chem. Phys. Lett. 382 (2004) 508–517.
[16] T.K. Mukherjee, P.P. Mishra, A. Datta, Chem. Phys. Lett. 407 (2005) 119–123.
[17] I. Gupta, M. Ravikanth, J. Org. Chem. 69 (2004) 6796–6811.
[18] L. Latos-Grazynski, in: K.M. Kadish, K.M. Smith, R. Guilard (Eds.), The Porphyrin Handbook, vol. 2, Academic Press, New York, 2000, pp. 361–416.
[19] D.C. Hilmey, M. Abe, M.I. Nelen, C.E. Stilts, G.A. Baker, S.W. Baker, F.V. Bright, S.R. Davies, S.O. Gollnick, A.R. Oseroff, S.L. Gibson, R. Hilf, M.R. Detty, J. Med. Chem. 45 (2002) 449–461.
[20] See the Supporting Information.
[21] N.C. Maiti, M. Ravikanth, S. Mazumdar, N. Periasamy, J. Phys. Chem. 99 (1995) 17192–17197.
[22] A.S.R. Koti, J. Tanija, N. Periasamy, Chem. Phys. Lett. 375 (2003) 171–176.
[23] S.C.M. Gandini, V.E. Yushmanov, I.E. Borissevitch, M. Tabak, Langmuir 15 (1999) 6233–6243.
[24] P.P. Mishra, J. Bhatnagar, A. Datta, Chem. Phys. Lett. 386 (2004) 158–161.

[25] R.F. Pasternack, C. Bustamante, P.J. Collings, E.J. Gibbs, J. Am. Chem. Soc. 115 (1993) 5393–5399.
[26] R.F. Pasternack, P.J. Collings, Science 269 (1995) 935–939.
[27] N.C. Maiti, S. Mazumdar, N. Periasamy, J. Phys. Chem. B 102 (1998) 1528–1538.
[28] H.L. Tavernier, A.V. Barzykin, M. Tachiya, M.D. Fayer, J. Phys. Chem. B 102 (1998) 6078–6088.
[29] K. Kalyansundaram, Photochemistry in Microheterogeneous Systems, Orlando, Academic, 1987.
[30] H. Sumi, R.A. Marcus, J. Chem. Phys. 84 (1986) 4894–4914.
[31] I.V. Rubstov, H. Shirota, K. Yoshihara, J. Phys. Chem. A 103 (1999) 1801–1808.
[32] S. Ghosh, K. Sahu, S.K. Mondal, P. Sen, K. Bhattacharyya, J. Chem. Phys. 125 (2006) 1–7, 054509.